Optical Characteristics of OTD Flashes and the Implications for Flash-Type Discrimination

W. J. KOSHAK

NASA Marshall Space Flight Center, Huntsville, Alabama

(Manuscript received 15 October 2009, in final form 30 April 2010)

ABSTRACT

Flashes detected by the Optical Transient Detector (OTD) that occur over the continental United States (CONUS) are intercompared with data from the National Lightning Detection Network (NLDN) in order to partition the OTD flashes into ground and cloud flashes. The entire 5-yr OTD dataset for CONUS is analyzed. The statistical distributions of a variety of optical characteristics are examined, including five flash-level attributes (radiance, area, duration, number of optical groups, and number of optical events), and two group-level attributes [the maximum number of events in a group (MNEG), and a closely related parameter, the maximum group area (MGA)]. On average, there were 5.6 optical groups per return stroke in a ground flash, which is in part due to the likelihood that OTD detects interstroke K changes. It was found that return strokes within ground flashes typically produce large optical groups; hence, the MNEG and MGA parameters serve as useful ''return-stroke detectors.'' The results of this study provide insight on how to construct an algorithm for retrieving the fraction of ground flashes in a set of flashes observed from a satellite lightning imager. Specifically, even though it is shown that the statistical distributions of the optical characteristics for ground and cloud flashes overlap substantially, the *mean values* of these distributions differ. Hence, a retrieval method that is based on an analysis of the distribution of the means, and that employs the central limit theorem of statistics, is recommended. As the sample size used to compute the means is increased, the overlap in the distributions of the means for ground and cloud flashes is diminished, making ground flash fraction retrieval feasible. Of the seven optical characteristics examined here, the mean MNEG and mean MGA parameters are suggested as being the most useful for discriminating between ground and cloud flashes in the context of this ''central limit theorem'' approach.

1. Introduction

In the early 1980s, observations and analyses of cloud-top lightning optical emissions provided important details on lightning optical pulse characteristics and statistics (Christian et al. 1983; Christian and Goodman 1987; Goodman et al. 1988). The optical data were collected using a National Aeronautics and Space Administration (NASA) U2 aircraft equipped with an optical pulse sensor (OPS) that employed a wide angle field-of-view lens. The data and associated statistical results became the central starting point for defining instrument specifications for space-based lightning imaging sensors.

In the statistical analyses by Goodman et al. (1988), which included Student's *t* tests of mean pulse width and pulse rise-time data, and a consideration of the earlier Monte Carlo modeling results of Thomason and Krider (1982), it was concluded that it would not be feasible to discriminate between ground and cloud flashes from geostationary orbit (based solely on optical data, and given the present generation of optical detectors). Until recently, no detailed flash-type (ground or cloud) discrimination feasibility studies were performed using data collected from the Optical Transient Detector (OTD; 1995–2000) and the Lightning Imaging Sensor (LIS; 1997–present). However, it was stated that an analysis of space-based very-high-frequency (VHF) signatures in tandem with optical data, as provided by the Fast On-Orbit Recording of Transient Events (FORTE), would greatly enhance a satellite's ability to discriminate lightning type, with the bulk of the discrimination capability being associated with the interpretation of FORTE VHF spectrograms (Suszcynsky et al. 2000). Hence, credit is due to

Corresponding author address: Dr. William Koshak, VP61, Earth Science Office, 320 Sparkman Drive, Robert Cramer Research Hall, NASA Marshall Space Flight Center, Huntsville, AL 35805.
E-mail: william.koshak@nasa.gov

DOI: 10.1175/2010JTECHA1405.1

the Suszcynsky et al. (2000) study for pioneering the idea of using both optical and VHF data in flash-type discrimination.

However, there is a desire to discriminate ground flashes from cloud flashes based solely on OTD/LIS optical measurements because similar observations will be made in geostationary orbit by the future Geostationary Operational Environmental Satellite (GOES)-R Geostationary Lightning Mapper (GLM). Therefore, lightning radiative transfer modeling within deep clouds has continued (Koshak et al. 1994; Light et al. 2001b; Davis and Marshak 2002), and comparisons between ground-based VHF lightning detection data and LIS data have been carried out (Thomas et al. 2000). Additional studies, many of which involve using the FORTE dataset, have also improved the physical understanding of cloud-top lightning optical emissions (Suszcynsky et al. 2001; Light et al. 2001a; Kirkland et al. 2001; Davis et al. 2002; Light and Jacobson 2002; Noble et al. 2004; Beasley and Edgar 2004). Credit is due to the study by Davis et al. (2002) for providing specific additional information on flash optical properties as a function of flash type, where the flash type is corroborated by the FORTE VHF data.

Note that by discriminating flash type, one can determine the ratio Z of the number of cloud flashes to the number of ground flashes. The Z ratio is thought to be particularly useful in a number of areas, including severe weather warning, lightning–convection relationships, lightning nitrogen oxide (NO_x) production, the contribution of lightning to the global electric circuit, and cross-sensor validation (see Boccippio et al. 2001).

An elevated positive polarity ground flash percentage has been linked to storm severity over specific regions of the continental United States (CONUS; Carey et al. 2003; Carey and Rutledge 2003). Hence, a better understanding of the relationships between the Z ratio, extreme weather events (e.g., tornado, hail, and strong wind gusts), and a positive ground flash percentage on monthly and seasonal time scales will provide insight into storm electrical, kinematic, and microphysical processes and their climatological variability.

The desire to obtain the Z ratio is particularly important to the atmospheric chemistry/climate modeling community. Presently, it is not well understood how to best model NO_x emissions from lightning because lightning discharges are highly variable. The peak current, channel length, channel altitude, stroke multiplicity, and number of flashes that occur in a particular region (i.e., flash density) all influence the amount of lightning NO_x produced. These five variables are not the same for ground and cloud flashes; for example, cloud flashes normally have lower peak currents, higher altitudes, and higher flash densities than ground flashes [see Koshak et al. (2009) for additional details]. Because existing satellite observations of lightning from the LIS and OTD do not distinguish between ground and cloud flashes, which produce different amounts of NO_x, it is very difficult to accurately account for the regional/global production of lightning NO_x. Hence, the ability to partition the LIS/OTD lightning climatology into separate ground and cloud flash distributions would substantially benefit the atmospheric chemistry modeling community. NO_x indirectly influences climate because it controls the concentration of ozone and hydroxyl radicals in the atmosphere. The importance of lightning-produced NO_x is emphasized throughout the scientific literature (e.g., Huntrieser et al. 1998). In fact, lightning is the most important NO_x source in the upper troposphere with a global production rate estimated to vary between 2 and 20 Tg(N) yr^{-1} (Lee et al. 1997), with more recent estimates of about 6 Tg(N) yr^{-1} (Martin et al. 2007). To make accurate predictions, global chemistry/climate models and regional air quality models must account for the effects of lightning NO_x more accurately. In particular, the NASA Goddard Institute for Space Studies (GISS) ModelE (Schmidt et al. 2006) and the Goddard Earth Observing System global chemical transport model (GEOS-CHEM; Bey et al. 2001) would each benefit from a ground–cloud flash partitioning of the LIS/OTD lightning climatology.

In this study, the 5-yr OTD dataset and associated National Lightning Detection Network (NLDN) data are reanalyzed to update and extend the preliminary study by Koshak (2007). Section 2 describes the data reduction methodology used to filter and partition the OTD flashes into ground and cloud flashes. Section 3 provides results of the statistical distributions of five flash-level optical characteristics (radiance, area, duration, number of events in a flash, number of groups in a flash) and two group-level characteristics [i.e., the maximum number of events in a group (MNEG) and a closely related observable, the maximum group area (MGA)]. Here, the basic terminology of OTD/LIS data is used; that is, a flash is composed of optical *groups*, and each optical group is composed of optical *events* (see Mach et al. 2007). The statistics are summarized and conclusions are drawn. An overall summary is provided in section 4. Though this study focuses on OTD data, similar analyses of LIS data are intended for future studies.

2. Data reduction

The study by Koshak (2007) provided frequency distributions of several optical properties of lightning observed by OTD for both ground and cloud flashes. The

partitioning of the (CONUS only) OTD data into separate ground and cloud flashes was achieved by comparing it to the NLDN ground flash data (which contain the time, location, peak current of the first return stroke, and the number of strokes in the ground flash). However, a more conservative reanalysis of the 5-yr CONUS OTD dataset is provided here in order to improve confidence in the partitioning accuracy. The present study also extends the preliminary study by Koshak (2007) to include the group-level attributes (MNEG and MGA).

a. Detection of CONUS flashes

Mean annual OTD flash densities as large as 35.4 flashes per square kilometer per year have been reported for North America (Christian et al. 2003). In addition, the NLDN detects millions of ground flashes over the CONUS each year (Huffines and Orville 1999). However, because OTD spent only a relatively small fraction of its time observing the CONUS in its orbit around the globe, it obviously does not capture all of the CONUS flashes. Note also that some flashes are not reported by OTD because of missing orbit files, or because the lightning cloud-top optical emission was too weak and did not break the OTD instrument detection threshold. Even if OTD triggers on a flash, it is still possible that it is (inadvertently) removed by the OTD data-processing algorithm. Accounting for all of these effects, a total of 490 445 flashes were captured by OTD over CONUS (which is crudely defined here as 25°–49° latitude, −125° to −67° longitude) during its 5-yr lifetime.

b. Classifying the OTD flashes

An OTD flash is classified in one of three ways: 1) a ground flash, 2) a cloud flash, or 3) an ambiguous flash. To decide what category an OTD flash belongs, two parameters are used. The first is the horizontal distance (or range) R between the OTD flash centroid and the NLDN event location. The second parameter is the time difference T between the time of the brightest group in the OTD flash and the time of an NLDN event. Note that the brightest group times are first adjusted appropriately for certain time delays before T is computed. That is, when intercomparing all OTD–NLDN times, a value of 2.6 ms is subtracted from the OTD time to approximately account for the total time lag of the optical signal from the source to OTD. This lag is composed of a pulse delay from the source to the cloud top of about 0.2 ms (200 μs) resulting from cloud multiple scattering (Koshak et al. 1994; Goodman et al. 1988), plus a transit time from cloud top to OTD of about 2.4 ms.

By specifying values of R and T, the OTD flashes can be categorized. An OTD flash is classified as a ground discharge if at least one NLDN event can be found such that $R \leq 50$ km and $T \leq 20$ ms both hold. The 50-km criterion is equivalent to the median OTD location error reported in Boccippio et al. (2000); this location error is primarily due to satellite navigation errors and, to a lesser extent, to OTD pixel resolution limitations. An OTD flash is conservatively classified as an ambiguous flash if the following two conditions are met: (i) it is *not* classified as a ground flash, and (ii) at least one NLDN event can be found such that $R \leq 200$ km and $T \leq 2$ s hold. Finally, an OTD flash is conservatively classified as a cloud flash if all NLDN events satisfy at least one of the following conditions: $R > 200$ km, $T > 2$ s.

There is a convenient way to visualize this classification scheme. The value R can be viewed as the radius, and $h \equiv 2|T|$ the height, of a right circular cylinder. The ground flashes are contained in the inner cylinder ($R = 50$ km, $h = 4$ ms), the ambiguous flashes are contained outside this inner cylinder but are inside an outer concentric cylinder ($R = 200$ km, $h = 4$ s), and all of the cloud flashes are contained outside of this outer concentric cylinder. The OTD flash centroid is located on the axis of the concentric cylinders, and the time of the brightest group is located on the midplane of the concentric cylinders.

Of the 490 445 OTD flashes, a total of 20 422 (4.2%) were classified as ground flashes, 215 050 (43.8%) were classified as cloud flashes, and 254 973 (52.0%) were classified as ambiguous. The percent classified as "ambiguous" is fairly large because a *conservative* partitioning has been intentionally applied. That is, the intent of this study is to provide statistical distributions on the optical characteristics of (just) ground flashes and (just) cloud flashes, not some mixture of ground and cloud flashes resulting from the incorrect classification of flash type. The ambiguous category allows a "buffer zone" that helps prevent against cross contamination of the ground and cloud flash samples.

c. Additional filtration

An OTD flash is rejected if it is associated with an alert flag (i.e., instrument alert flag, platform alert flag, external alert flag, processing and algorithm alert flag), if the flash did not pass routine quality assurance (QA) checks, or if the flash was classified as a noise event because the thunderstorm area count (TAC) was less than 140.

In addition, if an OTD flash is classified as a ground flash, a special filter applies. Previous investigators have recommended classifying positive NLDN flashes with peak currents less than 10 kA as cloud discharges (Cummins et al. 1998; Zajac and Rutledge 2001), and a 15-kA threshold has been more recently adopted (K. L. Cummins 2006, personal communication). Based

TABLE 1. Summary of OTD data classification and filtering.

Item	No. ground flashes		No. cloud flashes		Total	
Detected over CONUS	—		—		490 445	
Ambiguous flashes	—		—		254 973	
Unambiguous flashes	20 422		215 050		235 472	
QA alerts		−2480		−25 339		−27 819
TAC < 140		−135		−6635		−6770
Positive peak current < 15 kA		−922	—			−922
Outside mask		−4752		−75 830		−80 582
Inside mask	12 133		107 246		119 379	
Zero flash areas		−11		−80		−91
Final sample sizes	12 122		107 166		119 288	

on the study by Biagi et al. (2007) and Cummins and Murphy (2009), a 15-kA threshold is employed here. Hence, if an OTD flash is classified as a ground flash, but the associated NLDN event has a positive peak current less than 15 kA, the OTD flash is thrown out because it is suspected of being a cloud flash. Again, this is a conservative approach to minimize cross contamination between the final ground and cloud flash samples.

During the operational phase (1995–2000) of OTD, the NLDN detection efficiency and location accuracy degraded appreciably toward and outside of the U.S. borders and within certain parts of Texas, Florida, and New England (see Cummins et al. 1995). Therefore, a spatial filter (mask) was applied to the OTD data. Any flash occurring outside the mask was removed from this study because the NLDN data were compromised.

Table 1 summarizes all of the partitioning and filtering that is performed. Figure 1 provides a map of the spatial mask employed (in white); the locations of the 12 133 ground flashes are shown (red dots in top plot) and a total of 107 246 cloud flashes are shown (red dots in bottom plot). In some pathological cases, the OTD data-processing algorithm does not attempt to compute the flash areas, but rather assigns them to zero. Eleven such cases occurred in the ground flash sample, and 80 such cases occurred in the cloud flash sample. This gives the final sample sizes of 12 122 (ground flashes) and 107 166 (cloud flashes) shown in Table 1.

3. Results

a. Flash-level characteristics

Figure 2 provides the distributions of flash radiance and flash area for both ground (left column) and cloud (right column) flashes. In these, and similar plots to follow, the same ranges in the abscissa values have been used in order to facilitate ease in intercomparing the ground and cloud flash results. In addition, though statistics are provided for the entire sample sizes (12 122 ground flashes and 107 166 cloud flashes), the plots are truncated below the maximum value of the particular optical characteristic considered in order to better resolve the low end of the distribution, where the sample size is largest.

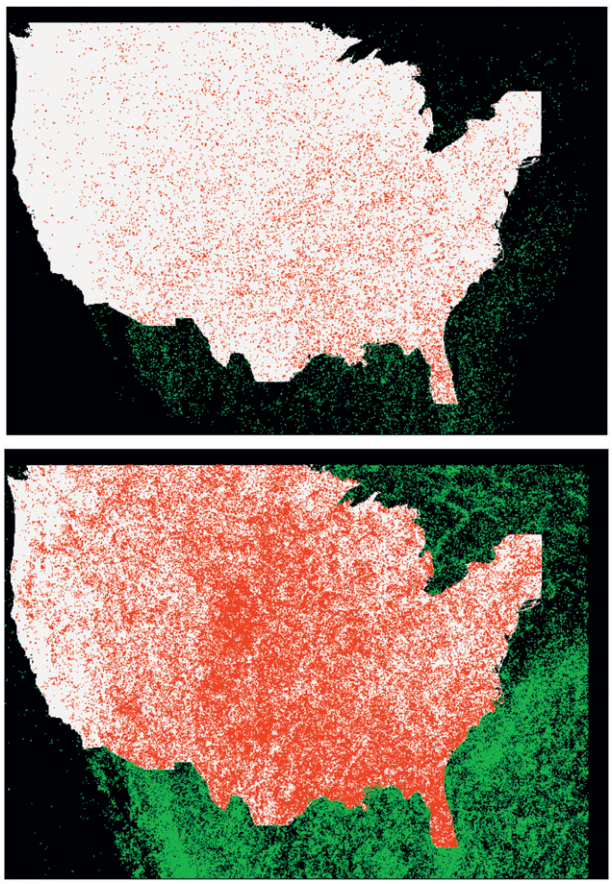

FIG. 1. (top) Spatial distribution of the 12 133 ground flashes (red dots) that had no QA alerts, no TAC < 140, and no positive peak currents below 15 kA; the 4752 green dots are ground flashes that also passed these filters but were removed because they fell outside of the spatial mask. (bottom) There are 107 246 cloud flashes (red dots) that had no QA alerts and no TAC < 140; a total of 75 830 cloud flashes are outside the mask (green dots).

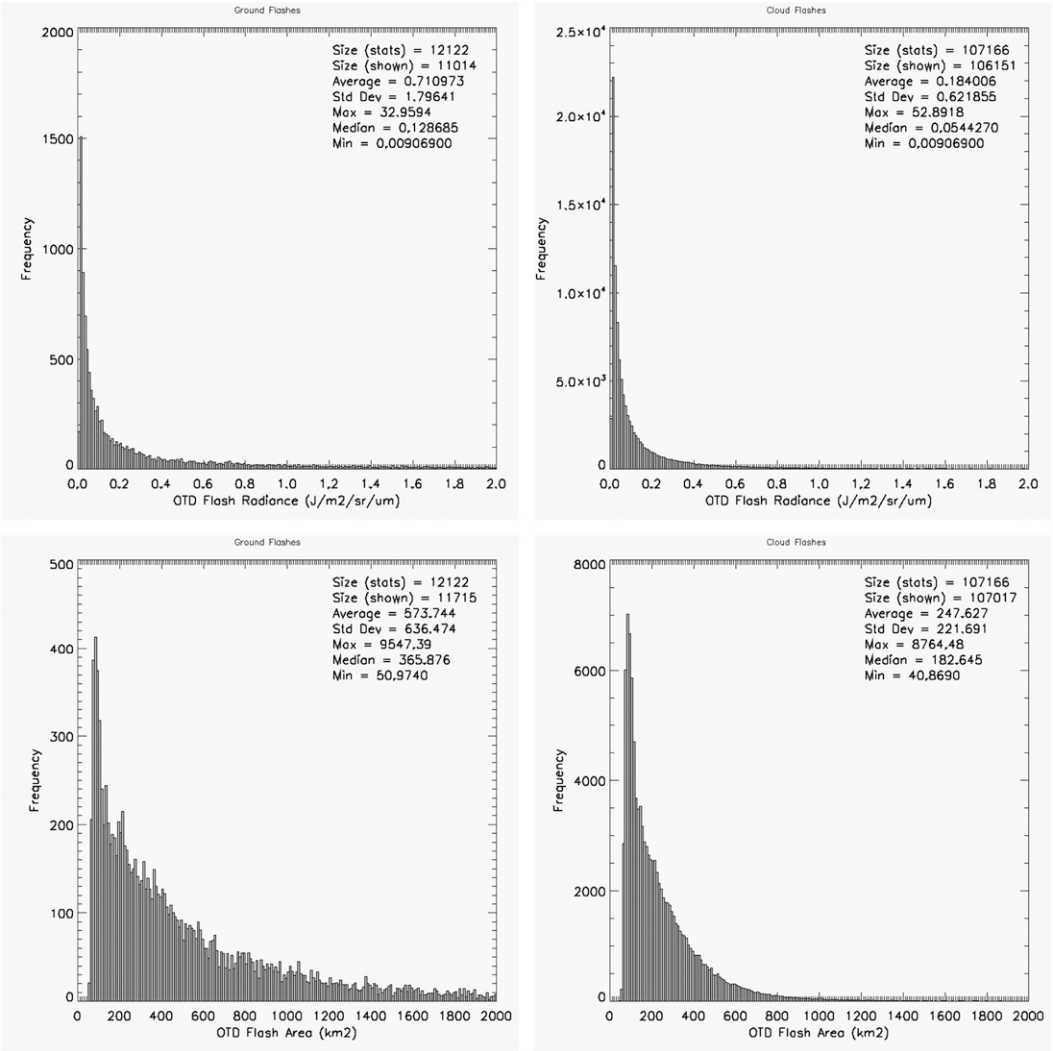

FIG. 2. The distributions of (top) flash radiance and (bottom) flash area for (left) ground flashes and (right) cloud flashes.

Figure 2 shows that the flash radiance distributions for the ground and cloud flashes overlap considerably. Hence, a straightforward (i.e., unsophisticated) application of flash radiance data would not be very useful for discriminating a ground flash from a cloud flash. (Because a detailed description of the OTD flash radiance data product is not provided in the literature, a detailed description is provided in the appendix; the description also fully applies to the LIS flash radiance product.) Similarly, the flash area distributions overlap appreciably.

Figure 3 provides the distributions of flash duration. Flash duration is defined as the time stamp of the last event in the flash minus the time stamp of the first event in a flash. The time stamp resolution of OTD is 2 ms (i.e., one instrument frame time), so if all of the events in a flash occur in one instrument frame, the flash duration is designated as ''zero'' seconds, assuming no timing errors. The top plots in Fig. 3 include all of the flashes and the bottom plots are the results when one removes the single frame (''zero'' duration) flashes. Again, there is considerable overlap in the ground and cloud flash distributions for this optical characteristic.

Figure 4 provides the distributions of the number of events in a flash (top plots) and the number of groups in a flash (bottom plots). Once again, there is considerable overlap in the ground and cloud flash distributions. Because the NLDN multiplicity data were also acquired for each ground flash, the distribution of the ratio of the number of groups to multiplicity is provided in Fig. 5. It is found that, on average, a ground flash has about 5.6 optical groups per return stroke. This large average ratio could be indicative of OTD-detected interstroke K changes.

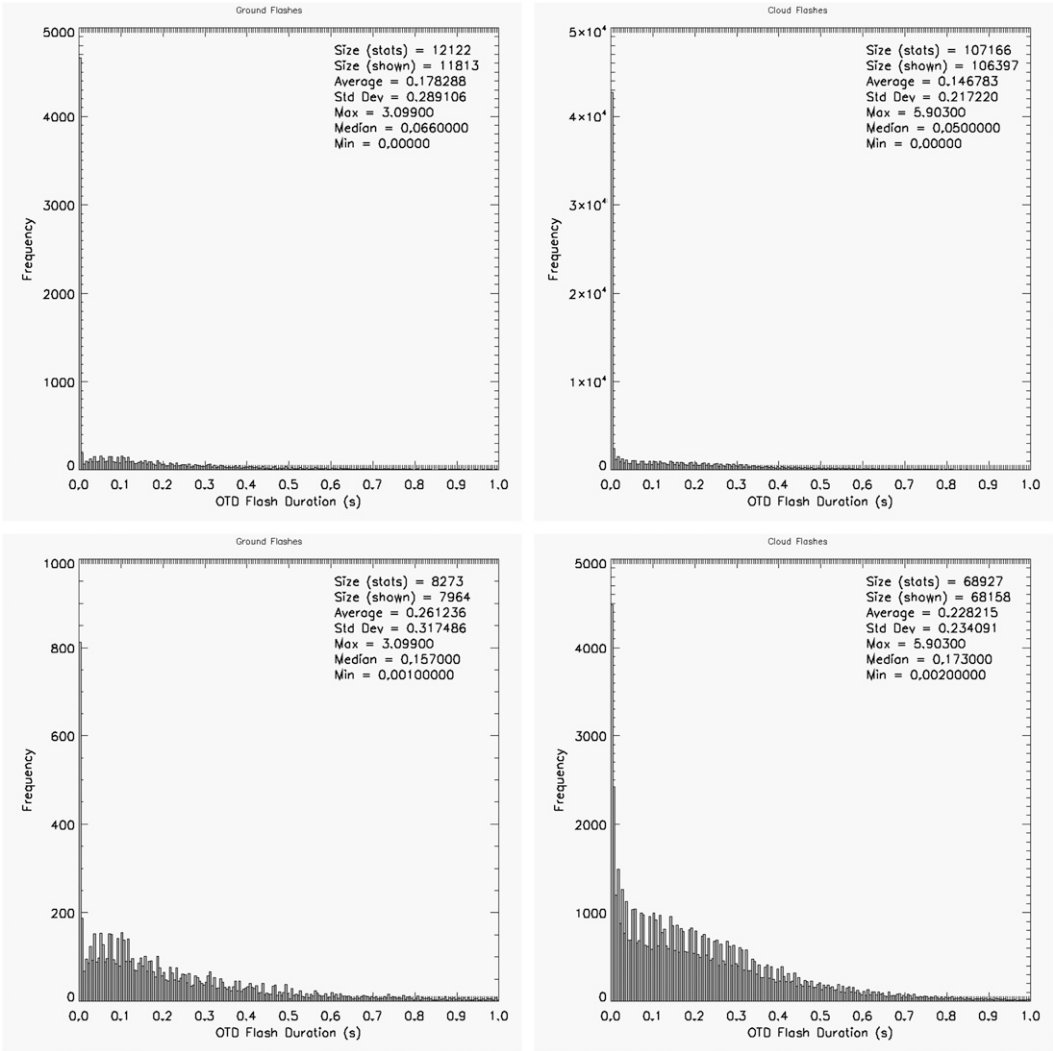

FIG. 3. The distributions of flash duration for (left) ground flashes and (right) cloud flashes. (bottom) The results when the ''zero'' duration (single frame flashes) are removed; see the text for a discussion.

However, the optical emissions from a single return stroke are not necessarily limited to a single OTD frame because of the effects of cloud multiple scattering, extensive return-stroke channel length development, and instrument frame splitting of the optical emission.

b. *Group-level characteristics*

Following the Koshak (2007) study, which also indicated overlap in the distributions of the five basic flash-level optical characteristics, it was desired to ''dig'' deeper into the OTD dataset to look for other optical characteristics that might help in flash-type discrimination. To do this, a user-friendly Interactive Data Language (IDL) widget software program, called FlashMovie, was developed. FlashMovie provides an easy way to scroll through the partitioned OTD dataset on a flash-by-flash basis in order to examine the spatiotemporal development of the cloud-top optical emissions. This ''bird's-eye'' view of each OTD flash over CONUS has been an effective tool for better understanding the emission process at the most resolved (optical event) level.

Figure 6 provides output from FlashMovie for a typical ground flash. The upper-left panel provides values of the five basic flash-level optical characteristics, the NLDN multiplicity, the ratio of the number of groups to the multiplicity, the NLDN peak current, and how separated the OTD flash was (in both space and in time) from the NLDN event. In the upper-right panel, FlashMovie provides the bird's-eye view of the flash optical emission as a movie (though obviously a time-integrated movie in this static plot). The plot in the lower-left panel shows the radiance of each event as a function of time,

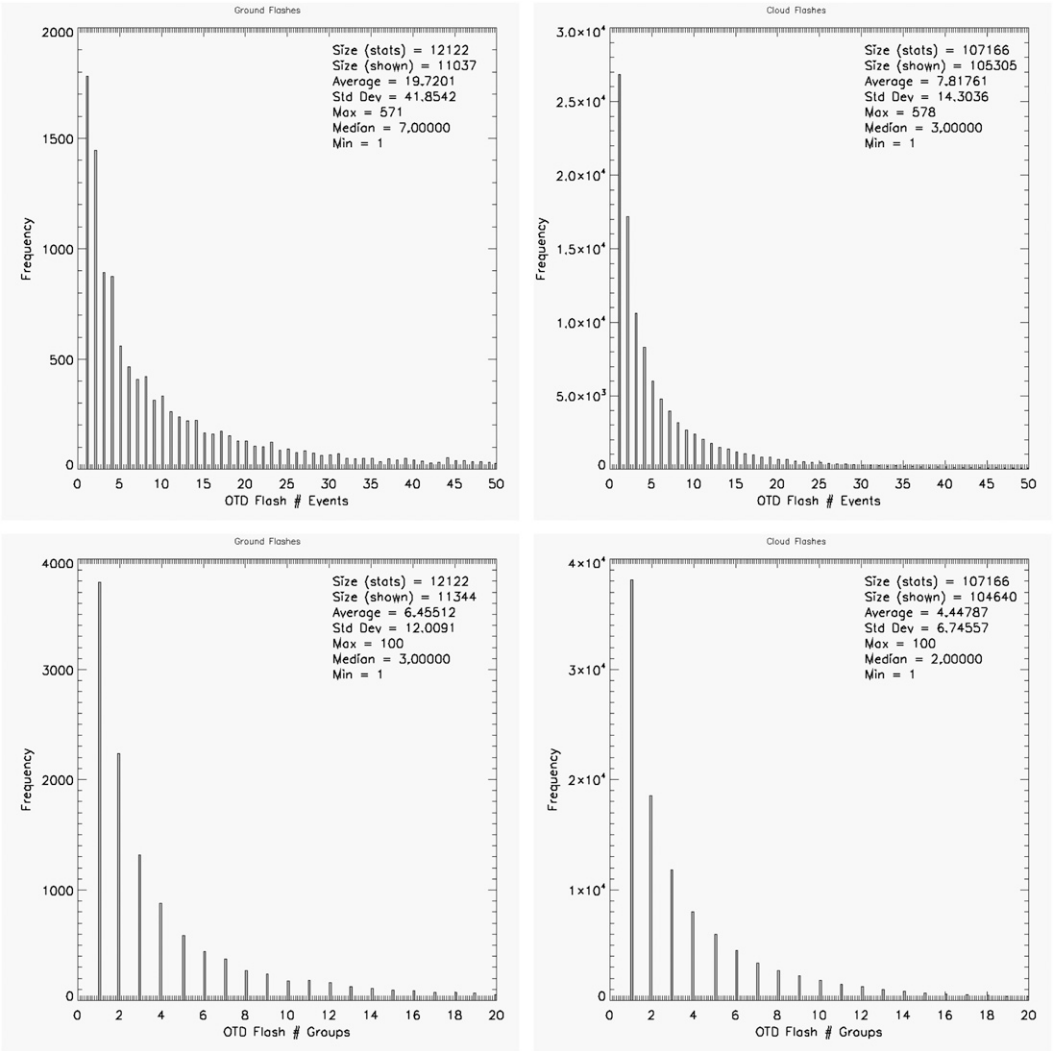

FIG. 4. The distributions of (top) the number of events in a flash and (bottom) the number of groups in a flash for (left) ground flashes and (right) cloud flashes.

and the lower-right panel shows the number of events in each instrument frame time (=2 ms) as a function of time. It is commonly found that most ground flashes have at least one frame with seven or more events (hence, the horizontal green line in the lower-right plot).

By comparison, cloud flashes commonly have no frames with seven or more events, as shown in Fig. 7. The plots in Figs. 6 and 7, and hundreds of others like them, are what have motivated the idea of using the maximum number of events in a frame (MNEF) as a fundamental parameter for distinguishing ground and cloud flashes. The MNEG and MGA parameters were chosen as a close proxy to MNEF. The difference between MNEF and MNEG is that it is possible to have more than one group in a single frame if the groupings are sufficiently separated in pixel space. The usefulness of MNEF and MNEG appear to be about the same, but because MNEG is slightly more convenient to extract from the OTD dataset, it has been used here. Overall, it was found that 28.1% of the ground flashes, and only 2.9% of the cloud flashes, had MNEG ≥ 7.

Finally, Fig. 8 shows an unusual cloud flash. Evidently, there were two source regions to the flash, and each region had an optical emission that ramped up slowly with time. This is much unlike the discrete ''comb function'' character presented in the two previous figures.

Because the MNEG and MGA variables have been useful in distinguishing ground flashes from cloud flashes, the distributions of these optical characteristics were found and are provided in Fig. 9. The ground and cloud flash means are encouragingly distinct, as discussed in the next section.

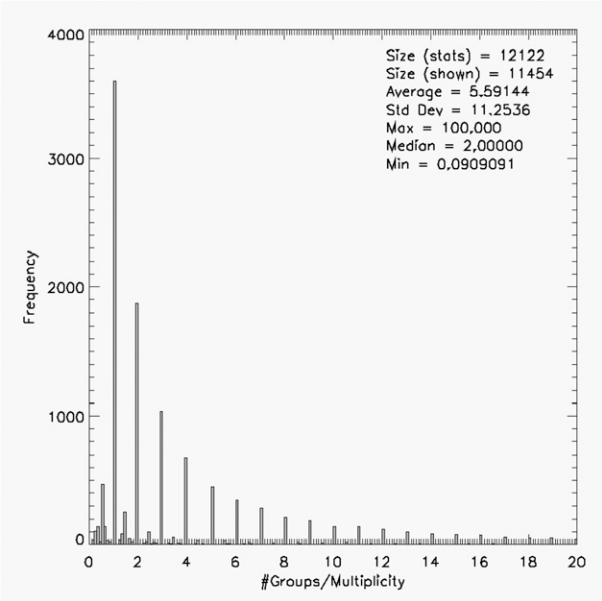

FIG. 5. The distribution of the ratio of the number of groups to the number of strokes in ground flashes. On average, there are nearly six groups per stoke in a ground flash, indicating that interstroke K changes are likely detected by OTD.

c. *Summary statistics and conclusions*

Table 2 shows a summary of the mean, median, and standard deviations of all seven optical characteristics analyzed in this study for both the ground and cloud flashes. Even though the ground and cloud flash distributions overlap appreciably, note from the ratios provided in the table that the mean and median optical characteristics are substantially larger for ground flashes than for cloud flashes.

Hence, suppose one observes N flashes from space that consist of a mixture of N_g ground flashes and N_c cloud flashes, that is, $N = N_g + N_c$. Also suppose that an optical characteristic, such as the MGA, is obtained for each of these N flashes. If N is a small number, say $N = 3$, then the mean MGA of these three observed flashes would provide very little information about the fraction of ground flashes N_g/N, because the distributions of the MGA for ground and cloud flashes (bottom plots in Fig. 9) overlap. However, if N is much larger, say $N > 30$, the distribution of the mean MGA must reasonably approximate a *normal distribution* pursuant to the central limit theorem (CLT) of statistics. Moreover, this normal distribution has a particular mean. Mathematically, if all flashes in the observable parent population were cloud flashes, then the mean of the normal distribution would approach the population mean MGA for cloud flashes (this population mean is estimated to be about 215.6 km^2 in Table 2). Conversely, if all flashes in the observable parent population were ground flashes, then the mean of the normal distribution would approach the population mean MGA for ground flashes (or about 493.0 km^2 in Table 2). Hence, in the general (i.e., actual) case of an arbitrary mixture of flashes, the mean of the normal distribution would sit between these two extremes and at a value dependent on the ground flash fraction. *In other words, the mean of the normal distribution shifts from the population mean characteristic of the cloud flashes to the population mean characteristic of the ground flashes as the ground flash fraction moves from zero to unity.* This mathematical effect is the key to ground flash fraction retrieval and is an inescapable consequence and benefit of the CLT.

To illustrate this point further, but from a slightly different viewpoint, one can independently examine the underlying ground and cloud flash characteristic. The upper-left panel of Fig. 10 provides two exponential distributions. Suppose the black curve represents the distribution of some optical characteristic x for cloud flashes and the red curve represents the distribution of the same optical characteristic, but for ground flashes. The vertical black and red lines denote the population mean values of the black and red distributions, respectively. Note that the two distributions overlap considerably so they are not very useful for straightforward flash-type discrimination purposes. However, when one plots the distribution of $\overline{x}$ for just the cloud flashes and the distribution of $\overline{x}$ for just the ground flashes, one obtains the black and red curves in the other five panels of Fig. 10; here, a mean value is based on a sampling of N^* observations of the optical characteristic. That is, one considers either N^* cloud flashes or N^* ground flashes, depending on what distribution (black or red) one is looking at in Fig. 10. Note that the overlap is quickly removed as N^* increases, provided that the population means (the vertical black and red lines) are distinct. Specifically, the CLT guarantees that as N^* increases, the distribution of the means approaches a normal distribution centered on the population mean (the vertical line) with standard deviation $\sigma/\sqrt{N^*}$, where σ is the standard deviation of the original ($N^* = 1$) distribution. The expression $\sigma/\sqrt{N^*}$ explicitly describes how the overlap is removed, because it defines the "half-width" of the resulting normal distribution. In addition, note that the CLT holds quite generally, that is, not just for exponential distributions, as shown in Fig. 10. Thus, again, if all flashes in the observable parent population were cloud flashes, then one would expect the value of the observed $\overline{x}$ (for $N^* = 100$) to be normally distributed about the vertical black line in the lower-right panel of Fig. 10. If all of the flashes in the observable parent population were ground flashes, then one would expect the value of the observed $\overline{x}$ (for $N^* = 100$) to be normally distributed

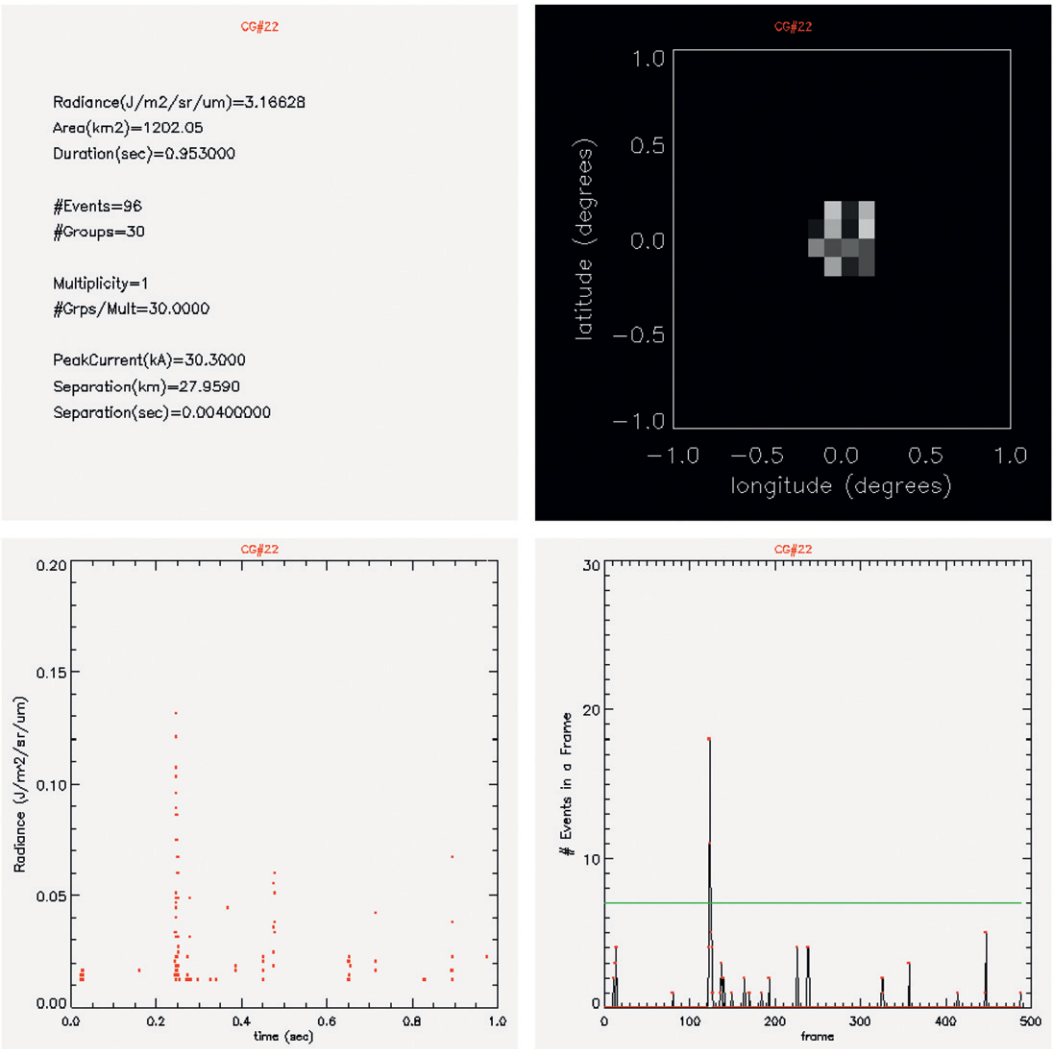

FIG. 6. Sample output from the IDL FlashMovie software for a typical OTD ground flash (see text for a discussion of the four-panel format). Ground flashes commonly have (bottom right) at least one frame with seven or more events (the horizontal green line threshold). (bottom) This particular ground flash had just one return stroke according to NLDN, and there is certainly a strong pulse as shown (pulse radiance of almost 0.14 J m^{-2} sr^{-1} μm^{-1} and 18 events in one frame). The instrument frame time is 2 ms, so the abscissa in each of the two bottom plots ranges from 0 to 1 s.

about the vertical red line in this same panel. The normal distributions in the lower-right panel of Fig. 10 provide the respective probability densities of $\bar{x}$ in each of these cases. Finally, and most importantly, if the observable parent population of flashes is a mixture of cloud and ground flashes (this is the general/actual case), then one would expect the observed $\bar{x}$ to be normally distributed about an intermediate value between the vertical black and red lines, with *the peak of the normal distribution being centered closer to the black line for a ground flash fraction near zero, and the peak being centered closer to the red line for a ground flash fraction near unity*. Clearly, the accuracy of such a ground flash fraction retrieval method improves as N increases.

Again, it is emphasized here that a flash-type discrimination method based on examining the distribution of the means of a particular optical characteristic, as suggested here, is obviously useful only for retrieving the *fraction* of ground flashes in a set of N flashes, and hence cannot be used to determine flash type on a flash-by-flash basis.

Some additional conclusions can be made from the results in Table 2. Note that the flash duration and the number of groups in a flash appear less useful for flash-type discrimination because these optical characteristics

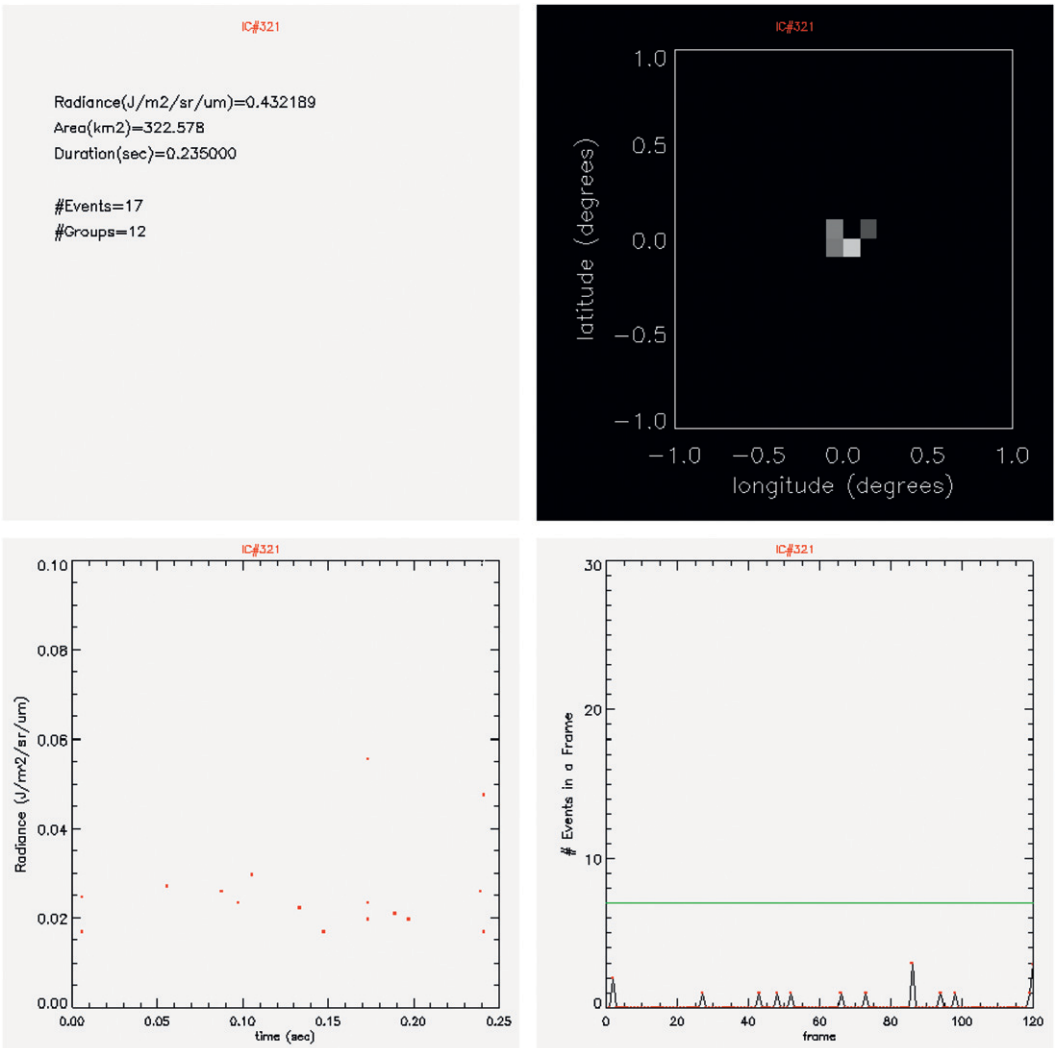

FIG. 7. Sample output from the IDL FlashMovie software for a typical OTD cloud flash. (bottom right) Cloud flashes commonly have no frames with seven or more events (the horizontal green line threshold).

have the smallest ratios in the table. Conversely, flash radiance has the largest ratio, but the standard deviations of the flash radiances are quite large. Dividing the standard deviation of the flash radiance by the mean flash radiance gives 1.796/0.711 = 2.53 for the ground flashes and 0.622/0.184 = 3.38 for the cloud flashes. Repeating this computation for the other optical characteristics in Table 2, one finds that flash radiance has the largest standard deviations (relative to the means) than any of the other optical characteristics examined. For successful flash-type discrimination, one desires just the opposite, that is, a small standard deviation relative to the mean. Note that the MNEG variable has a large ground/cloud ratio (2.49 for the ratio of the means), and yet a reasonably small standard deviation relative to the mean (i.e., 6.610/5.726 = 1.15 for ground flashes and 1.947/2.301 = 0.846 for cloud flashes). In addition, as described in the previous subsection, MNEG also serves as a good "return-stroke detector." Therefore, it is suggested that the *mean* MNEG of a sample of *N* lightning imager observations would be highly useful for flash-type discrimination; for the same reasons, the *mean* MGA would also be quite useful for flash-type discrimination.

4. Summary

This study has made an effort to determine what optical characteristics commonly observed by a satellite lightning imager, such as the OTD/LIS or future GLM, would be most useful for discriminating ground flashes from cloud flashes. Five flash-level optical characteristics (radiance, area, duration, number of events, and

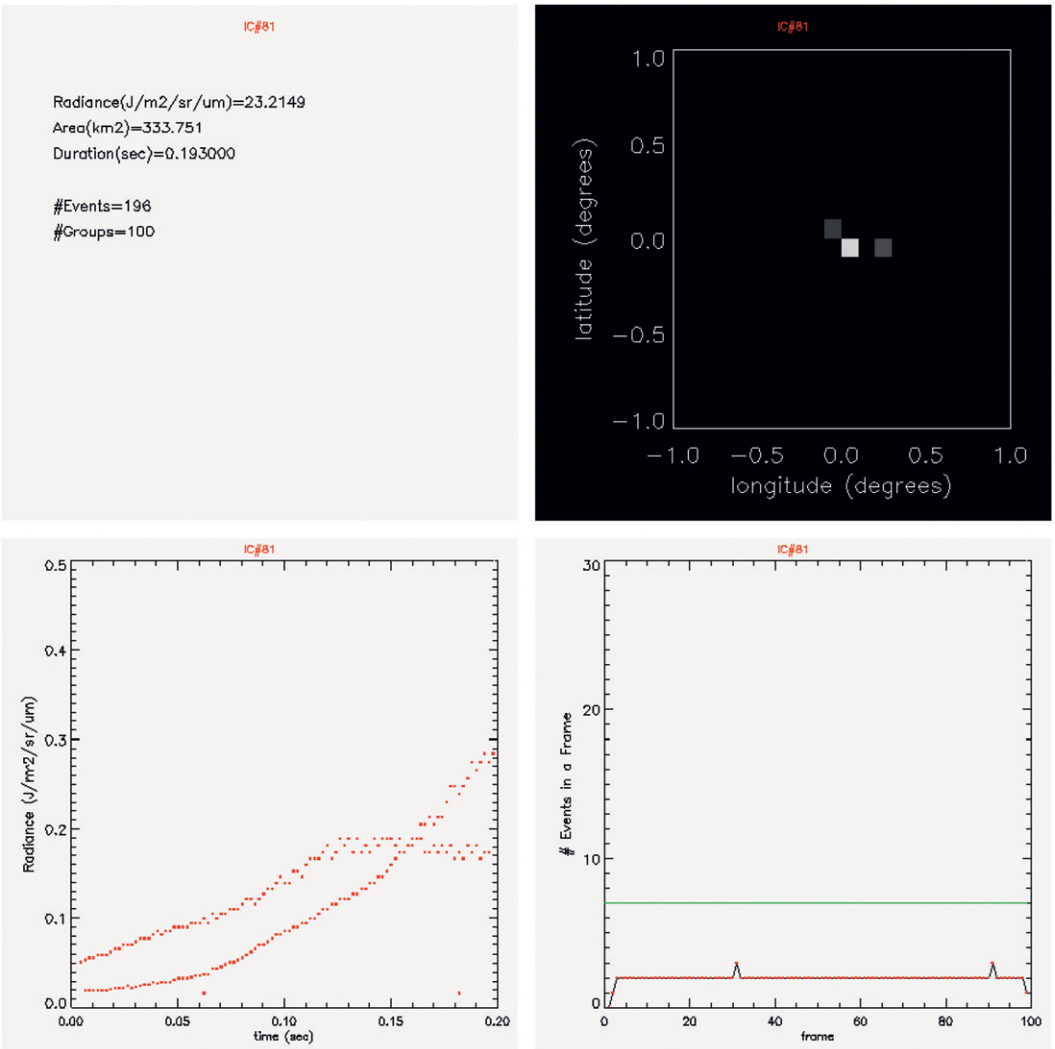

FIG. 8. Sample output from the IDL FlashMovie software for a very atypical OTD cloud flash. There apparently were two source regions to the flash whose optical emissions each ramped up slowly (but distinctly) with time. This smooth pattern is much unlike the discrete ''comb function'' character presented in the two previous figures.

number of groups), and two group-level characteristics [the maximum number of events in a group (MNEG), and the maximum group area (MGA)] were examined.

The reason for examining the MNEG and MGA group-level characteristics came from a detailed study of individual OTD flashes. IDL FlashMovie software was developed to examine the individual OTD flashes at the flash, group, and event levels. The software provided a ''bird's-eye'' view movie loop of the spatiotemporal evolution of each flash, with simultaneous time series plots of the number of optical events in each 2-ms instrument frame. From these detailed movie loops and the available NLDN data, it was determined that MNEG and MGA are useful ''return-stroke detectors.'' In fact, 28.1% of the ground flashes, and only 2.9% of the cloud flashes, had MNEG ≥ 7.

The entire 5-yr OTD dataset was analyzed to obtain all of the OTD flashes detected over CONUS. These data were then partitioned into ground and cloud flashes using NLDN data, and then meticulously filtered to ensure a properly classified subpopulation of cloud and ground flashes. The partitioning strategy was highly conservative in order to minimize cross contamination; that is, a set of pure ground flashes and a set of pure cloud flashes were sought because any mixing of the two would contaminate the final statistical distributions of the ground and cloud flash optical properties.

The statistical distributions of all seven optical characteristics (five flash level and two group level) were provided for the ground and cloud flashes. The ground flash distribution was shown to overlap considerably with

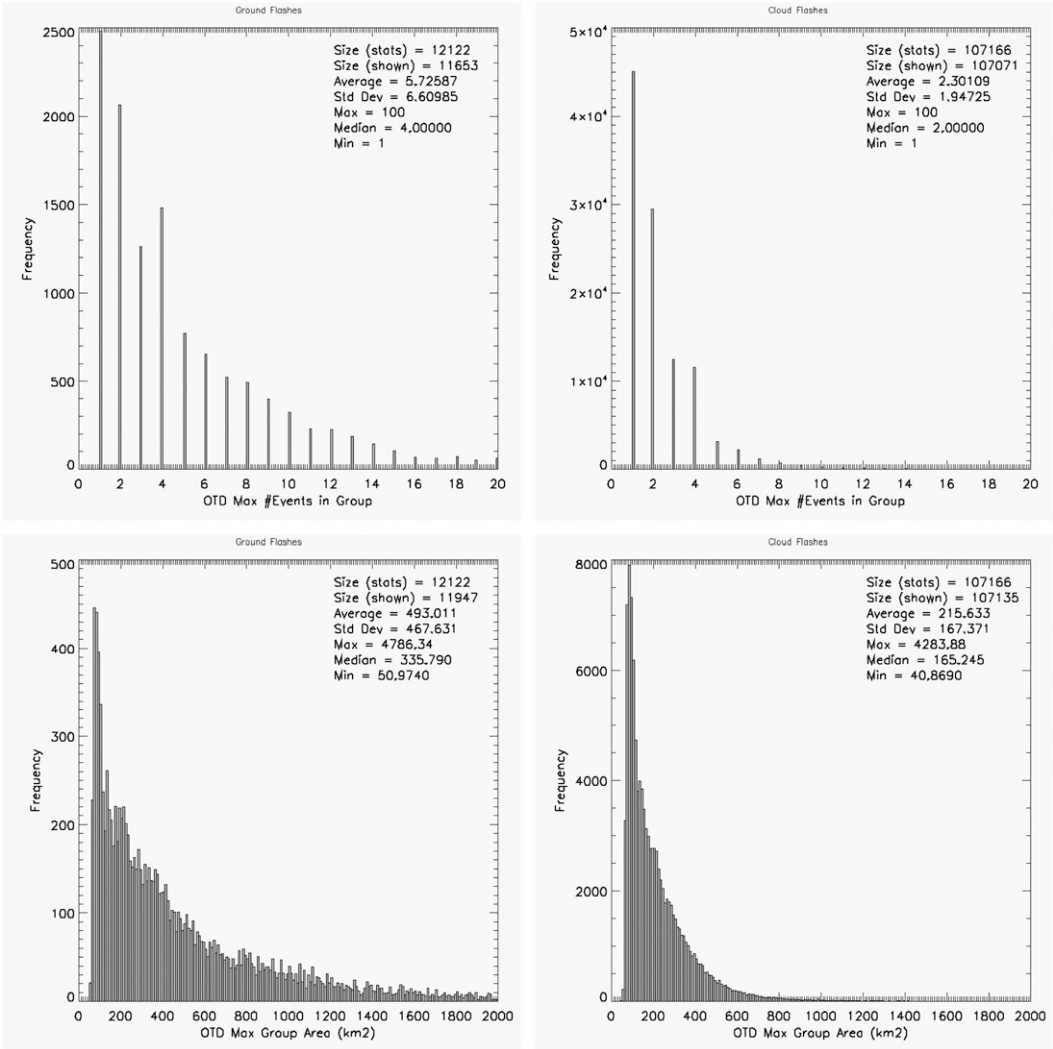

FIG. 9. The distribution of (top) MNEG and (bottom) MGA for (left) ground flashes and (right) cloud flashes.

the cloud flash distribution for each of the seven optical characteristics, but the means, medians, and standard deviations were distinct.

Hence, it was suggested that a ground flash fraction retrieval algorithm could be based on the *distributions of the means*, rather than on the distributions themselves. Whereas the overlapping distributions of a ground and cloud flash optical characteristic make flash-type discrimination difficult, the relatively small overlap in the distributions of the means makes ground flash fraction

TABLE 2. A summary of the mean, median, and standard deviation ratios.

Optical characteristic	Ground			Cloud			Ratio (ground/cloud)		
	Mean	Median	Std dev	Mean	Median	Std dev	Mean	Median	Std dev
Flash radiance (J m^{-2} sr^{-1} μm^{-1})	0.711	0.129	1.796	0.184	0.054	0.622	3.86	2.39	2.89
Flash area (km)	573.744	365.876	636.474	247.627	182.645	221.691	2.32	2.00	2.87
Flash duration (s)	0.178	0.066	0.289	0.147	0.050	0.217	1.21	1.32	1.33
Flash No. events (dimensionless)	19.720	7.000	41.854	7.818	3.000	14.304	2.52	2.33	2.93
Flash No. groups (dimensionless)	6.455	3.000	12.009	4.448	2.000	6.746	1.45	1.50	1.78
MNEG (dimensionless)	5.726	4.000	6.610	2.301	2.000	1.947	2.49	2.00	3.39
MGA (km)	493.011	335.790	467.631	215.633	165.245	167.371	2.29	2.03	2.79

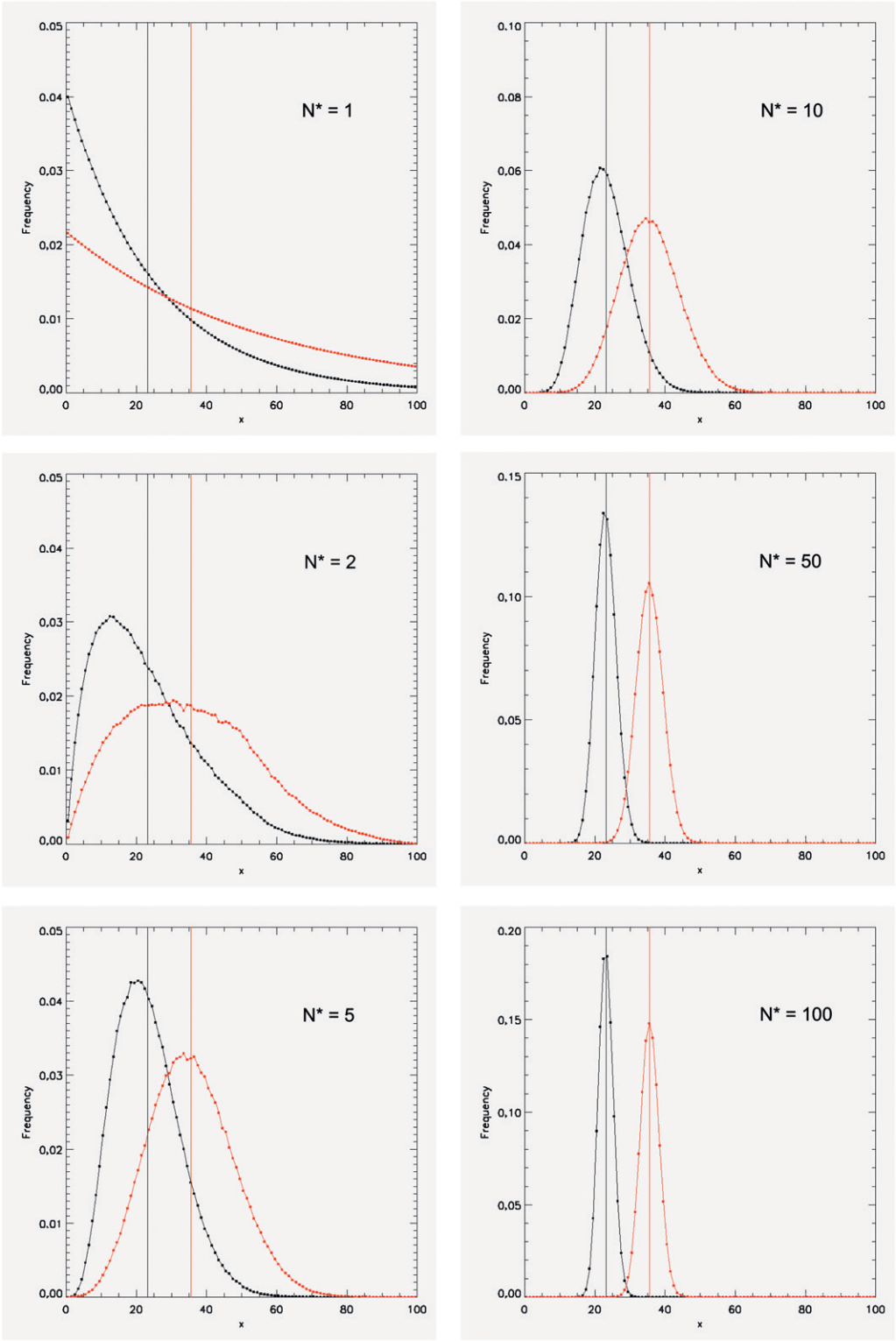

FIG. 10. Example of using the central limit theorem of statistics to transform two overlapping distributions [(top) $N^* = 1$] into two separated normal distributions [(bottom) $N^* = 100$] that are more useful for flash-type discrimination. The value of N^* is the number of samples (either of just ground or just cloud flashes) used to compute a mean optical characteristic. The vertical lines are the means of the two original distributions in the top left panel.

retrieval feasible. In particular, the central limit theorem of statistics can be exploited to remove most of the residual overlap in the distributions of the means by simply increasing the number of observations over which a mean optical characteristic is computed. The method discussed here is useful only for retrieving the fraction of ground flashes in a set of N flashes, and cannot be used to determine flash type on a flash-by-flash basis. Nonetheless, as discussed in the introduction, the Z ratio (which is easily/algebraically obtained from the ground flash fraction) would have important applications and benefits to both the OTD/LIS lightning climatology and future GLM observations.

Finally, because of the return-stroke detector properties of MGA and MNEG, and because the mean values of these parameters differ appreciably between ground and cloud flashes, the *means* of MGA and MNEG were recommended as being the most useful for ground flash fraction retrieval. Indeed, the key to retrieving the ground flash fraction (a variable having a value between zero and unity) is that it is related to the average of MGA (or MNEG), which is easily derived from the set of N satellite-observed flashes; these flashes being a mixture of ground and cloud flashes.

Acknowledgments. This research has been supported by the NOAA/NESDIS/STAR GOES-R Risk Reduction Program under Memorandum of Agreement NA07AANEG0284 [Ms. Ingrid Guch, Chief, NOAA/NESDIS/STAR Cooperative Research Programs Division; Dr. Mark DeMaria Chief, NOAA/NESDIS Regional and Mesoscale Meteorology Branch; and Dr. Steven J. Goodman, Senior (Chief) Scientist, GOES-R System Program], and by the LIS project (Program Manager, Ramesh Kakar, NASA Headquarters) as part of the NASA Earth Science Enterprise (ESE) Earth Observing system (EOS) project. The author would also like to thank Dr. Richard Solakiewicz of Chicago State University for helping to identify a more conservative flash partitioning strategy than that employed in Koshak (2007), and for his comments on improving the final draft manuscript. Thanks are also given to Dr. Dennis Boccippio (NASA/MSFC) for providing a convenient form of the 5-yr OTD dataset. Finally, thanks are given to Mr. Dennis Buechler of the University of Alabama-Huntsville for his suggestions on how best to implement the spatial mask lightning filter.

APPENDIX

The Flash Radiance Data Product

In section 3, the distribution of the OTD "flash radiance" data product P_λ^* is provided. Technically however, this data product is not really a flash radiance, but rather only a proxy to flash radiance. In this section, a precise definition of P_λ^* in terms of familiar radiometric quantities is offered. The discussion also directly applies to the LIS flash radiance data product.

a. Preliminary definitions and derived quantities

Given an optical emission like a lightning flash, the spectral radiance $R_\lambda = R_\lambda(\mathbf{r}, \hat{\Omega}, t)$ detected by an observer depends on the observer's location $\mathbf{r}$; the direction the observer is looking $\hat{\Omega} = \hat{\Omega}(\theta, \varphi)$, where (θ, φ) are polar and azimuth angles, respectively; and on the time t of observation. The variable λ is the wavelength, and the units of R_λ are W m^{-2} sr^{-1} μm^{-1}. Because one is interested in the spectral radiance observed by OTD, $\mathbf{r} = \mathbf{r}_o(t)$, where $\mathbf{r}_o(t)$ is the location of the center of the OTD entrance aperture and is a known vector function of time related to the satellite emphemeris and attitude. Eliminating $\mathbf{r}$ in favor of t gives the spectral radiance $I_\lambda = I_\lambda(\hat{\Omega}, t)$ impinging on the OTD entrance aperture.

The OTD instrument frame time τ is 2 ms. This consists of a 1.9-ms integration time during which the impinging optical radiation is collected, plus an additional 0.1-ms frame transfer time during which the radiation can get "smeared" across pixels as their charge values are being read out. By design, errors resulting from frame transfer are small, that is, under 0.1 ms/1.9 ms = 5.3%.

Suppose that only one flash occurs within the OTD field of view, that it is completely within the field of view, and that it subtends a solid angle $\Delta\Omega$ as viewed from OTD, that is, as viewed at location $\mathbf{r}_o(t)$. Let us also assume that the flash occupies $i = 1, \ldots, m$ frames, where the ith frame begins at time t_{i-1} and ends at time t_i, and $\tau = t_i - t_{i-1} = 2$ ms. The spectral energy density $\xi_\lambda(\hat{\Omega}, i)$ (in units of J m^{-2} sr^{-1} μm^{-1}) impinging on the OTD entrance aperture from direction $\hat{\Omega}$ that is collected during the ith frame is defined as

$$\xi_\lambda(\hat{\Omega}, i) \equiv \int_{t_{i-1}}^{t_i} I_\lambda(\hat{\Omega}, t)\, dt. \tag{A1}$$

In general, the flash of solid angle $\Delta\Omega$ illuminates $j = 1, \ldots, n$ pixels and the solid angle subtended at the sensor by the jth pixel footprint is given by $\Delta\omega_j$. Therefore, the flash solid angle can be discretized as

$$\Delta\Omega = \sum_{j=1}^{n} \Delta\omega_j. \tag{A2}$$

Thus, the spectral radiance and (single frame) spectral energy density averaged over the flash solid angle $\Delta\Omega$ are, respectively,

$$\langle I_\lambda(\hat{\Omega}, t)\rangle \equiv \frac{1}{\Delta\Omega}\int_{\Delta\Omega} I_\lambda(\hat{\Omega}, t)\, d\Omega,$$
$$\langle \xi_\lambda(\hat{\Omega}, i)\rangle \equiv \frac{1}{\Delta\Omega}\int_{\Delta\Omega} \xi_\lambda(\hat{\Omega}, i)\, d\Omega, \tag{A3}$$

and the same variables averaged over the jth pixel footprint of solid angle $\Delta\omega_j$ are

$$\bar{I}_{\lambda j}(t) \equiv \frac{1}{\Delta\omega_j}\int_{\Delta\omega_j} I_\lambda(\hat{\Omega}, t)\, d\Omega,$$
$$\bar{\xi}_{\lambda j}(i) \equiv \frac{1}{\Delta\omega_j}\int_{\Delta\omega_j} \xi_\lambda(\hat{\Omega}, i)\, d\Omega. \tag{A4}$$

Because of (A1), one also has the relations

$$\langle \xi_\lambda(\hat{\Omega}, i)\rangle = \int_{t_{i-1}}^{t_i} \langle I_\lambda(\hat{\Omega}, t)\rangle\, dt,$$
$$\bar{\xi}_{\lambda j}(i) = \int_{t_{i-1}}^{t_i} \bar{I}_{\lambda j}(t)\, dt. \tag{A5}$$

Because the integrals in (A3) can be rewritten as a sum of integrals, that is,

$$\int_{\Delta\Omega} (\ )\, d\Omega \ \rightarrow\ \sum_{j=1}^{n}\int_{\Delta\omega_j} (\ )\, d\Omega, \tag{A6}$$

(A4) can be used to rewrite the expressions in (A3) as

$$\langle I_\lambda(\hat{\Omega}, t)\rangle = \frac{1}{\Delta\Omega}\sum_{j=1}^{n}\Delta\omega_j \bar{I}_{\lambda j}(t),$$
$$\langle \xi_\lambda(\hat{\Omega}, i)\rangle = \frac{1}{\Delta\Omega}\sum_{j=1}^{n}\Delta\omega_j \bar{\xi}_{\lambda j}(i). \tag{A7}$$

b. Two fundamental quantities

Because the flash duration is $\Delta t = t_m - t_o$ and occupies $i = 1, \ldots, m$ frames, the total spectral energy density received from direction $\hat{\Omega}$ during flash time Δt is

$$\xi_\lambda(\hat{\Omega}) \equiv \int_{t_o}^{t_m} I_\lambda(\hat{\Omega}, t)\, dt = \sum_{i=1}^{m}\int_{t_{i-1}}^{t_i} I_\lambda(\hat{\Omega}, t)\, dt = \sum_{i=1}^{m} \xi_\lambda(\hat{\Omega}, i). \tag{A8}$$

Averaging (A8) over the flash solid angle $\Delta\Omega$ and using the second equation in (A7) gives

$$\langle \xi_\lambda(\hat{\Omega})\rangle = \left\langle \sum_{i=1}^{m} \xi_\lambda(\hat{\Omega}, i)\right\rangle = \sum_{i=1}^{m}\langle \xi_\lambda(\hat{\Omega}, i)\rangle$$
$$= \frac{1}{\Delta\Omega}\sum_{i=1}^{m}\sum_{j=1}^{n}\Delta\omega_j \bar{\xi}_{\lambda j}(i). \tag{A9}$$

The quantity $\langle \xi_\lambda(\hat{\Omega})\rangle$ is important because it represents the solid angle–averaged spectral energy density intercepted by OTD resulting from the flash of duration Δt. Another important quantity is the total spectral energy per area (J m^{-2} μm^{-1}) intercepted by OTD, call it u_λ, given by

$$u_\lambda \equiv \int_{t_o}^{t_m}\int_{\Delta\Omega} I_\lambda(\hat{\Omega}, t)\, d\Omega\, dt = \sum_{i=1}^{m}\sum_{j=1}^{n}\Delta\omega_j \bar{\xi}_{\lambda j}(i). \tag{A10}$$

The last result is obtained by using the first equation in (A4) and the second equation in (A5), and by rewriting the integrals as sums over ith frames and jth pixels. Comparing (A9) and (A10) allows one to link the two fundamental quantities as follows:

$$u_\lambda = \langle \xi_\lambda(\hat{\Omega})\rangle \Delta\Omega. \tag{A11}$$

c. OTD flash radiance data product

Consider the following proxy variable P_λ [the simple sum of the mean spectral energy densities across each illuminated pixel from each frame (J m^{-2} sr^{-1} μm^{-1})]:

$$P_\lambda \equiv \sum_{i=1}^{m}\sum_{j=1}^{n}\bar{\xi}_{\lambda j}(i) = \sum_{i=1}^{m}\sum_{k=1}^{n_i}\bar{\xi}_{\lambda k}(i). \tag{A12}$$

Here, note that n_i is the number of pixels in the ith frame that are illuminated by the flash, and n is the total number of pixels that are illuminated by the flash. The two sums are necessarily equivalent because $\bar{\xi}_{\lambda j}(i) = 0$ when the jth pixel is *not* illuminated by the flash during the ith frame.

The OTD "flash radiance" data product is

$$P_\lambda^* = \sum_{i=1}^{m}\sum_{k=1}^{n_i}\bar{\xi}_{\lambda k}^*(i) + \sum_{i=1}^{m}\sum_{l=1}^{N_i}\varepsilon_{\lambda l}(i). \tag{A13}$$

Here, N_i is the number of pixels in the ith frame that are *not* illuminated by the flash. The (threshold modified) average spectral energy density for the jth pixel illuminated in the ith frame $\bar{\xi}_{\lambda j}^*(i)$ and the (threshold modified) false alarm spectral energy density $\varepsilon_{\lambda l}(i)$ are given by

$$\bar{\xi}_{\lambda k}^*(i) = \bar{\xi}_{\lambda k}(i) + e_{\lambda k}(i) + T_{\lambda k}(i),$$
$$\varepsilon_{\lambda l}(i) = e_{\lambda l}(i) + T_{\lambda l}(i). \tag{A14}$$

Note that the OTD measurement errors are described by $e_{\lambda k}(i)$, and the effect of employing a threshold setting is described by $T_{\lambda k}(i)$. For example, if the instrument measurement $\bar{\xi}_{\lambda k}(i) + e_{\lambda k}(i)$ is below the instrument threshold setting, then $T_{\lambda k}(i) = -\bar{\xi}_{\lambda k}(i) - e_{\lambda k}(i)$ such that $\bar{\xi}_{\lambda k}^*(i) = 0$; otherwise, $T_{\lambda k}(i) = 0$. Similarly, given that the lth pixel in the ith frame is not illuminated, if the

instrument measurement error $e_{\lambda l}(i)$ is below the instrument threshold setting, then $T_{\lambda l}(i) = -e_{\lambda l}(i)$, such that $\varepsilon_{\lambda l}(i) = 0$; otherwise, $T_{\lambda l}(i) = 0$ and a false alarm occurs. Note also that the OTD flash radiance data product is not technically a radiance value, but rather a spectral energy density; however, this was the vernacular used in describing the data product within the OTD software distribution. Plugging (A14) into (A13) gives

$$P_\lambda^* = \sum_{i=1}^{m}\sum_{k=1}^{n_i}\bar{\xi}_{\lambda k}(i) + \left[\sum_{i=1}^{m}\sum_{k=1}^{n_i}\{e_{\lambda k}(i) + T_{\lambda k}(i)\} + \sum_{i=1}^{m}\sum_{l=1}^{N_i}\{e_{\lambda l}(i) + T_{\lambda l}(i)\}\right] \equiv P_\lambda + E_\lambda, \tag{A15}$$

where (A12) was used, and the term in the square brackets is defined as the total spectral error E_λ. Hence, if one assumes that $\Delta\omega_j \cong \Delta\omega = \text{const}$, then $\Delta\Omega \cong n\Delta\omega$, $u_\lambda \cong \Delta\omega \sum_{i=1}^{m}\sum_{j=1}^{n}\bar{\xi}_{\lambda j}(i)$, and the data product can be readily written in terms of the well-known radiometric quantities derived in the previous section, that is,

$$P_\lambda^* \cong \frac{1}{\Delta\omega}u_\lambda + E_\lambda = n\langle\xi_\lambda(\hat{\Omega})\rangle + E_\lambda. \tag{A16}$$

This is the desired result. It clearly indicates how the OTD flash radiance data product is related to familiar quantities [the total intercepted spectral energy per area u_λ and the average spectral flash energy density $\langle\xi_\lambda(\hat{\Omega})\rangle$].

REFERENCES

Beasley, W. H., and B. C. Edgar, 2004: Early coincident satellite optical and ground-based RF observation of lightning. *Geophys. Res. Lett.,* **31,** L07107, doi:10.1029/2003GL018991.

Bey, I., and Coauthors, 2001: Global modeling of tropospheric chemistry with assimilated meteorology: Model description and evaluation. *J. Geophys. Res.,* **106,** 23 073–23 095.

Biagi, C. J., K. L. Cummins, K. E. Kehoe, and E. P. Krider, 2007: National Lightning Detection Network (NLDN) performance in southern Arizona, Texas, and Oklahoma in 2003–2004. *J. Geophys. Res.,* **112,** D05208, doi:10.1029/2006JD007341.

Boccippio, D. J., and Coauthors, 2000: The Optical Transient Detector (OTD): Instrument characteristics and cross-sensor validation. *J. Atmos. Oceanic Technol.,* **17,** 441–458.

——, K. L. Cummins, H. J. Christian, and S. J. Goodman, 2001: Combined satellite- and surface-based estimation of the intracloud-cloud-to-ground lightning ratio over the continental United States. *Mon. Wea. Rev.,* **129,** 108–122.

Carey, L. D., and S. A. Rutledge, 2003: Characteristics of cloud-to-ground lightning in severe and nonsevere storms over the central United States from 1989–1998. *J. Geophys. Res.,* **108,** 4483, doi:10.1029/2002JD002951.

——, ——, and W. A. Petersen, 2003: The relationship between severe storm reports and cloud-to-ground lightning polarity in the contiguous United States from 1989 to 1998. *Mon. Wea. Rev.,* **131,** 1211–1228.

Christian, H. J., and S. J. Goodman, 1987: Optical observations of lightning from a high-altitude airplane. *J. Atmos. Oceanic Technol.,* **4,** 701–711.

——, R. L. Frost, P. H. Gillaspy, S. J. Goodman, O. H. Vaughan Jr., M. Brook, B. Vonnegut, and R. E. Orville, 1983: Observations of optical lightning emissions from above thunderstorms using U-2 aircraft. *Bull. Amer. Meteor. Soc.,* **64,** 120–123.

——, and Coauthors, 2003: Global frequency and distribution of lightning as observed from space by the Optical Transient Detector. *J. Geophys. Res.,* **108,** 4005, doi:10.1029/2002JD002347.

Cummins, K. L., and M. J. Murphy, 2009: An overview of lightning locating systems: History, techniques, and data uses, with an in-depth look at the U.S. NLDN. *IEEE Trans. Electromagn. Compat.,* **51,** 499–518.

——, E. A. Bardo, W. L. Hiscox, R. B. Pyle, and A. E. Pifer, 1995: NLDN'95: A combined TOA/MDF technology upgrade of the U.S. National Lightning Detection Network. *Extended abstracts, Int. Aerospace and Ground Conf. on Lightning and Static Electricity,* Williamsburg, VA, National Interagency Coordination Group, 72-1–72-15.

——, M. J. Murphy, E. A. Bardo, W. L. Hiscox, R. B. Pyle, and A. E. Pifer, 1998: A combined TOA/MDF technology upgrade of the U.S. National Lightning Detection Network. *J. Geophys. Res.,* **103,** 9035–9044.

Davis, A. B., and A. Marshak, 2002: Space-time characteristics of light transmitted through dense clouds: A Green's function analysis. *J. Atmos. Sci.,* **59,** 2713–2727.

Davis, S. M., D. M. Suszcynsky, and T. E. L. Light, 2002: FORTE observations of optical emissions from lightning: Optical properties and discrimination capability. *J. Geophys. Res.,* **107,** 4579, doi:10.1029/2002JD002434.

Goodman, S. J., H. J. Christian, and W. D. Rust, 1988: A comparison of the optical pulse characteristics of intracloud and cloud-to-ground lightning as observed above clouds. *J. Appl. Meteor.,* **27,** 1369–1381.

Huffines, G. R., and R. E. Orville, 1999: Lightning ground flash density and thunderstorm duration in the continental United States: 1989–96. *J. Appl. Meteor.,* **38,** 1013–1019.

Huntrieser, H., H. Schlager, C. Feigl, and H. Holler, 1998: Transport and production of NO_x in electrified thunderstorms: Survey of previous studies and new observations at mid-latitudes. *J. Geophys. Res.,* **103,** 28 247–28 264.

Kirkland, M. W., D. M. Suszcynsky, J. L. L. Guillen, and J. L. Green, 2001: Optical observations of terrestrial lightning by the FORTE satellite photodiode detector. *J. Geophys. Res.,* **106** (D24), 33 499–33 509.

Koshak, W. J., 2007: OTD observations of continental US ground and cloud flashes. *Proc. 13th Int. Conf. on Atmospheric Electricity,* Beijing China, International Commission on Atmospheric Electricity, 823–826. [Available online at http://hdl.handle.net/2060/20070038268.]

——, R. J. Solakiewicz, D. D. Phanord, and R. J. Blakeslee, 1994: Diffusion model for lightning radiative transfer. *J. Geophys. Res.,* **99,** 14 361–14 371.

——, M. N. Khan, A. P. Biazar, M. Newchurch, and R. T. McNider, 2009: A NASA model for improving the lightning NO_x emission inventory for CMAQ. Preprints, *Fourth Conf. on the Meteorological Applications of Lightning Data and the 11th*

Conf. on Atmospheric Chemistry, Phoenix, AZ, Amer. Meteor. Soc., J8.2. [Available online at http://ams.confex.com/ams/pdfpapers/147334.pdf.]

Lee, D. S., and Coauthors, 1997: Estimations of global NO_x emissions and their uncertainties. *Atmos. Environ.,* **31,** 1735–1749.

Light, T. E., and A. R. Jacobson, 2002: Characteristics of impulsive VHF lightning signals observed by the FORTE satellite. *J. Geophys. Res.,* **107,** 4756, doi:10.1029/2001JD001585.

——, D. M. Suszcynsky, and A. R. Jacobson, 2001a: Coincident radio frequency and optical emissions from lightning, observed with the FORTE satellite. *J. Geophys. Res.,* **106** (D22), 28 223–28 231.

——, ——, M. W. Kirkland, and A. R. Jacobson, 2001b: Simulations of lightning optical waveforms as seen through clouds by satellites. *J. Geophys. Res.,* **106** (D15), 17 103–17 114.

Mach, D. M., H. J. Christian, R. J. Blakeslee, D. J. Boccippio, S. J. Goodman, and W. L. Boeck, 2007: Performance assessment of the Optical Transient Detector and Lightning Imaging Sensor. *J. Geophys. Res.,* **112,** D09210, doi:10.1029/2006JD007787.

Martin, R. V., B. Sauvage, I. Folkins, C. E. Sioris, C. Boone, P. Bernath, and J. Ziemke, 2007: Space-based constraints on the production of nitric oxide by lightning. *J. Geophys. Res.,* **112,** D09309, doi:10.1029/2006JD007831.

Noble, C. M. M., W. H. Beasley, S. E. Postawko, and T. E. L. Light, 2004: Coincident observations of lightning by the FORTE photodiode detector, the New Mexico Tech Lightning Mapping Array and the NLDN during STEPS. *Geophys. Res. Lett.,* **31,** L07106, doi:10.1029/2003GL018989.

Schmidt, G. A., and Coauthors, 2006: Present-day atmospheric simulations using GISS ModelE: Comparison to in-situ, satellite, and reanalysis data. *J. Climate,* **19,** 153–192.

Suszcynsky, D. M., M. W. Kirkland, A. R. Jacobson, R. C. Franz, S. O. Knox, J. L. L. Guillen, and J. L. Green, 2000: FORTE observations of simultaneous VHF and optical emissions from lightning: Basic phenomenology. *J. Geophys. Res.,* **105** (D2), 2191–2201.

——, T. E. Light, S. Davis, J. L. Green, J. L. L. Guillen, and W. Myre, 2001: Coordinated observations of optical lightning from space using the FORTE photodiode detector and CCD imager. *J. Geophys. Res.,* **106** (D16), 17 897–17 906.

Thomas, R. J., P. R. Krehbiel, W. Rison, T. Hamlin, D. J. Boccippio, S. J. Goodman, and H. J. Christian, 2000: Comparison of ground-based 3-dimensional lightning mapping observations with satellite-based LIS observations in Oklahoma. *Geophys. Res. Lett.,* **27,** 1703–1706.

Thomason, L., and E. Krider, 1982: The effects of cloud on the light produced by lightning. *J. Atmos. Sci.,* **39,** 2051–2065.

Zajac, B. A., and S. A. Rutledge, 2001: Cloud-to-ground lightning activity in the contiguous United States from 1995 to 1999. *Mon. Wea. Rev.,* **129,** 999–1019.